Numerical Method for Modeling of Acoustic Waves Propagation

Sławomir DYKAS, Włodzimierz WRÓBLEWSKI,
Sebastian RULIK, Tadeusz CHMIELNIAK

Silesian University of Technology
Institute of Power Engineering and Turbomachinery
Konarskiego 18, 44-100 Gliwice, Poland
e-mail: slawomir.dykas@polsl.pl

In this paper, numerical results of modeling of acoustic waves propagation are presented. For calculation of the acoustic fluctuations, a solution of the full non-linear Euler equation is used. The Euler equations are solved with the use of a numerical scheme of third-order accuracy in space and time. The paper shows a validation process of the described method. This method is suitable also for an aerodynamic noise assessment on the basis of unsteady mean flow field data obtained from a CFD calculations. In such case this method is called a hybrid CFD/CAA method. The proposed method is numerically decoupled with CFD solution, therefore the information about the mean unsteady flow field can be obtained using an arbitrary CFD method (solver). The accuracy of the acoustic field assessment depends on the quality of the CFD solutions. This decomposition reduces considerably the computational cost in comparison with direct noise calculations.

The presented Euler acoustic postprocessor (EAP) has been used for modeling of the acoustic waves propagation in a cavity and in the flow field around a cylinder and an aerodynamic profile.

Keywords: acoustic wave, fluctuation, aerodynamic noise, Euler equations.

Notations

Symbol

A – amplitude,
D – diameter,
f – frequency,
Ma – Mach number,
p – pressure,
t – time,
u, v, w – velocity components,

x, y, z – Cartesian coordinates,
     ρ – density.

Index

     0 – mean value from CFD calculations,
     $'$ – acoustic fluctuation.

Abbreviations

   CAA – Computational Aeroacoustics,
   CFD – Computational Fluid Dynamics,
   DNS – Direct Numerical Simulation,
   LES – Large Eddy Simulation,
   RMS – Root Mean Square,
   SPL – Sound Pressure Level,
 uRANS – unsteady Raynolds Averaged Navier-Stokes.

1. Introduction

In connection with a fast development of the computer technologies in the last two decades, the Computational Fluid Dynamics (CFD) has stopped confining to the use of the Raynolds Averaged Navier-Stokes (RANS) equations in modeling of the 3D flow field. Now, the methods for a prediction of an unsteady flow field, such as uRANS, the Large Eddy Simulation (LES) or even the Direct Numerical Simulation (DNS), play a dominant role in CFD modeling. These methods allow to obtain the instantaneous values, which can include some information about an acoustic fluctuation as well. It affected the development of a new branch of CFD called the Computational Aeroacoustics (CAA).

At present, the CAA methods become a more and more efficient tool for an aerodynamic noise prediction, for the aeroacoustic waves propagation and for identification of the noise sources. Due to the new, more restricted norms regarding the noise emission, the aerodynamic noise modeling (CAA) became one of the major goals of the aviation and automotive industry.

An intensive development of the numerical methods and computer technology allowed to make the acoustic research more effective and attractive in comparison with the experimental ones. The application of DNS methods for an aerodynamic noise prediction is still under academic consideration. Recently, the LES techniques are extensively developed for CAA problems, but it is still very time-consuming for the engineering applications. The CAA techniques are split mainly into two steps: determination of the flow field (CFD methods) and computation of the aerodynamic noise. These techniques are called the hybrid CFD/CAA methods. For prediction of the unsteady flow field, both the LES and uRANS simulations can be used (PRANTLE, 2002; SORGÜVEN, 2004). Majority of uRANS methods cannot capture the small Eddies, which usually produce a broadband noise. On the other hand, the Large Eddy Simulation, which

can capture majority of the turbulent scales, is usually too costly e.g. for turbomachinery applications. In this case, the hybrid uRANS/LES methods could constitute a compromise. In commercial applications, the Detached Eddy Simulation (DES) and Scale Adaptive Simulation (SAS) hybrid uRANS/LES methods are widely used. Generally, both the SAS and DES should give very similar results, but there are important differences between these two models. SAS is based on improved uRANS formulation that allows resolving of the turbulent spectrum in unstable flow conditions. On the other hand, DES is a combination of the RANS and LES methods. The switch between both methods is achieved by comparison of the modelled turbulent length scale and the grid spacing. Both the SAS and DES methods are available in commercial software ANSYS CFX.

Usually, for estimation of the aerodynamic noise, the acoustic analogy (Sorgüven, 2004) or solution of the Euler equations (Dykas *et al.*, 2006a, 2006b; Tam, 1995) for the acoustic variables are used. These two groups of CAA methods require some information about acoustic source or data concerning unsteady mean flow. The method presented, called the Euler acoustic postprocessor (EAP), is based on the solution of the full non-linear Euler equations for fluctuations and can be used for modeling of the acoustic waves propagation in arbitrary flow field.

By means of the presented method it is possible to estimate the aerodynamic noise data in a near field as well as in a far field. In the internal flows, an assessment of the noise sources is more important than modeling of a noise propagation. A reduction of the noise sources influences the flow efficiency and formation of vibrations. For turbomachinery applications, a special attention is paid to the noise generation by vortex structures behind the trailing edge of the blade and by the unsteady shock waves. The purpose of this work is to show the robustness of the presented method for such types of numerical modeling.

Many numerical methods used in CFD codes can not be applied for CAA methods, because they are too dissipative. It is obvious, that the acoustic waves are characterized by a much lower amplitudes and higher frequency than the pressure waves, but the use of 3rd accuracy order seems to be sufficient, what was confirmed in this paper by comparison with analytical solutions.

2. Numerical model

For description of the aerodynamic noise generation and propagation in the mean flow, the full nonlinear Euler equations have been chosen. These equations are formulated using decomposition of the actual variables into the mean flow parts ($_0$) and fluctuating parts ($'$). The conservative acoustic variables were in this case defined as:

$$\rho' = \rho - \rho_0,$$

$$(\rho u)' = (\rho u) - \rho_0 u_0,$$

$$(\rho v)' = (\rho v) - \rho_0 v_0, \tag{1}$$

$$(\rho w)' = (\rho w) - \rho_0 w_0,$$

$$(\rho E)' = (\rho E) - \rho_0 E_0,$$

In the Cartesian coordinates, full Euler equations have a form:

$$\frac{\partial \mathbf{Q}}{\partial t} + \frac{\partial \mathbf{E}}{\partial x} + \frac{\partial \mathbf{F}}{\partial y} + \frac{\partial \mathbf{G}}{\partial z} = 0, \tag{2}$$

where vector of conservative variables and fluxes can be written as follows:

$$\mathbf{Q} = \begin{bmatrix} \rho' \\ (\rho u)' \\ (\rho v)' \\ (\rho w)' \\ (\rho E)' \end{bmatrix},$$

$$\mathbf{E} = \begin{bmatrix} (\rho u)' \\ (\rho u)' \, u' + p' + \rho_0 u_0 u' + (\rho u)' \, u_0 \\ (\rho v)' \, u' + \rho_0 v_0 u' + (\rho v)' \, u_0 \\ (\rho w)' \, u' + \rho_0 w_0 u' + (\rho w)' \, u_0 \\ ((\rho E)' + p') \, u' + \rho_0 E_0 u' + (\rho E)' \, u_0 \end{bmatrix},$$

$$\mathbf{F} = \begin{bmatrix} (\rho v)' \\ (\rho u)' \, v' + \rho_0 u_0 v' + (\rho u)' \, v_0 \\ (\rho v)' \, v' + p' + \rho_0 v_0 v' + (\rho v)' \, v_0 \\ (\rho w)' \, v' + \rho_0 w_0 v' + (\rho w)' \, v_0 \\ ((\rho E)' + p') \, v' + \rho_0 E_0 v' + (\rho E)' \, v_0 \end{bmatrix},$$

$$\mathbf{G} = \begin{bmatrix} (\rho w)' \\ (\rho u)' \, w' + \rho_0 u_0 w' + (\rho u)' \, w_0 \\ (\rho v)' \, w' + \rho_0 v_0 w' + (\rho v)' \, w_0 \\ (\rho w)' \, w' + p' + \rho_0 w_0 w' + (\rho w)' \, w_0 \\ ((\rho E)' + p') \, w' + \rho_0 E_0 w' + (\rho E)' \, w_0 \end{bmatrix}.$$

The relations for the primitive fluctuating variables in function of the conservative fluctuating variables and mean values can be written in the form:

$$u' = \frac{(\rho u)' + \rho_0 u_0}{\rho' + \rho_0} - u_0,$$

$$v' = \frac{(\rho v)' + \rho_0 v_0}{\rho' + \rho_0} - v_0,$$

$$w' = \frac{(\rho w)' + \rho_0 w_0}{\rho' + \rho_0} - w_0, \tag{3}$$

$$p' = (\gamma - 1) \left[(\rho E)' - \frac{1}{2} \left(\rho_0 u_0 u' + (\rho u)' u_0 + (\rho u)' u_0 \right) \right.$$
$$\left. - \frac{1}{2} \left(\rho_0 v_0 v' + (\rho v)' v_0 + (\rho v)' v_0 \right) - \frac{1}{2} \left(\rho_0 w_0 w' + (\rho w)' w_0 + (\rho w)' w_0 \right) \right].$$

The detailed description of the presented Euler acoustic postprocessor, together with the applied numerical methods, have been done in our previous works (DYKAS *et al.*, 2006a, 2006b, 2008).

3. Calculation results

For validation of the presented numerical model many test cases have been used. Majority of them dealt with propagations of the acoustic waves in a mean flow. The main fundamental test for such phenomena is modeling of a 2D acoustic pulse propagation (see e.g. TAM, 1995). Initial Gaussian distribution pulse propagating in the mean flow can be evaluated in an analytical way. Such analytical solution is very good for validation of the numerical scheme.

In Fig. 1 the acoustic pressure distributions for one position in time have been presented. This test is crucial for future calculations and decides on the numerical mesh size. The acoustic pulse has been propagated in uniform mean flow. The Mach number in the mean flow amounted to 0.5. The numerical results have been compared with an analytical solution. It was shown (DYKAS, 2006b), that in order to model correctly the acoustic waves propagation by means of presented numerical method, at least 5 mesh points for the wave length have to be used. These test cases have been useful to check the implemented non-reflective boundary conditions as well.

The presented numerical method has also been used to calculate the noise propagations generated by a speaker and cavity (WEYNA, 2005). The cavity is located behind the speaker at a distance of ~0.4 m. The cavity depth is 0.45 m and width is 0.2 m (Fig. 2). The mean flow field velocity is set to 0 m/s and any disturbance is caused by the acoustic waves only. The non-reflective boundary conditions were applied for the upper boundary and for the inlet and outlet.
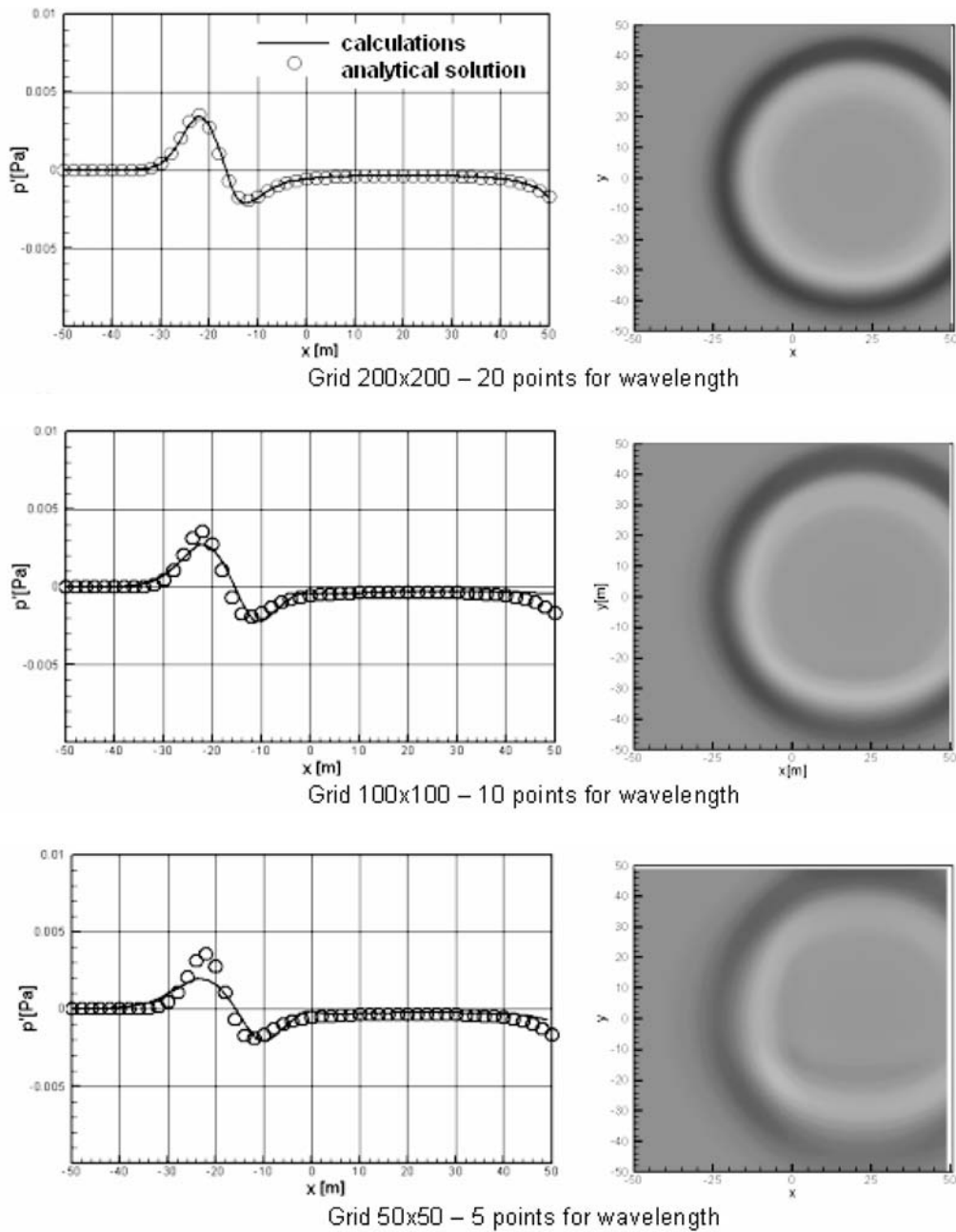
Fig. 1. Comparison of the calculated acoustic pressure distribution with analytical solution. Instantaneous acoustic pressure for time $t = 2 \times 0.0586$ s (Ma = 0.5).

The computational domain (Fig. 2) consists of 7 blocks and has about 0.3 mln nodes. The speaker is simulated by a time-dependent boundary condition. The
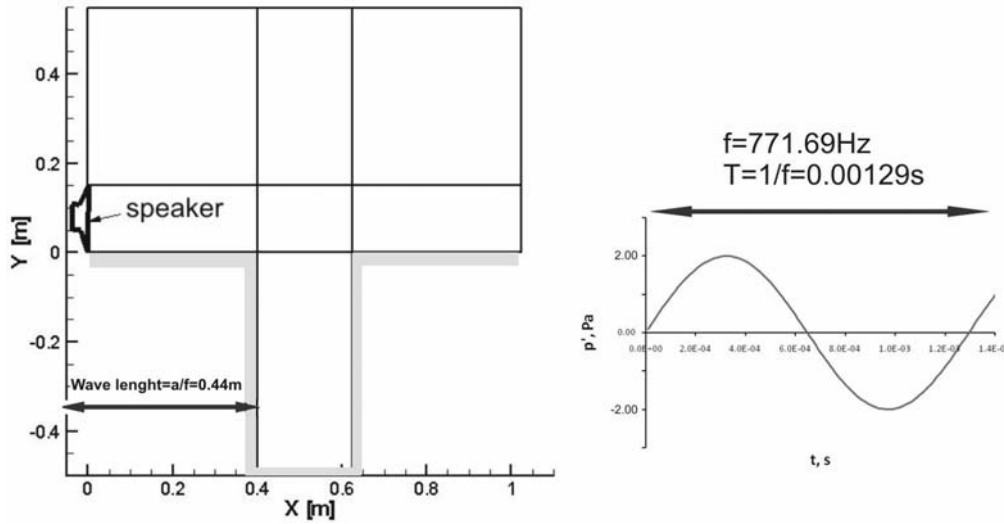
Fig. 2. Calculation domain and time-dependent boundary condition applied for the calculation.

acoustic pressure emitted by a speaker in this case is a function of time and is described by a wave equation:

$$p(t) = A \cdot \cos(2\pi f t). \tag{4}$$

In our case an amplitude (A) of the acoustic pressure was 2 Pa. The maximum value of 2 Pa corresponds to the sound pressure level of 100 dB. The frequency (f) in this case is constant and set to 771.69 Hz.

Figure 3 presents the five instantaneous states of the acoustic waves propagating in the analyzed domain. There is visible an interaction of the acoustic waves with the cavity.

In Fig. 4 the sound pressure level distribution is calculated as a Root Means Square of 10 instantaneous states for one period, according to the relations:

$$p'_{\text{rms}} = \sqrt{\frac{1}{n} \sum_{i=1}^{n=10} p_i'^2}, \tag{5}$$

$$\text{SPL} = 20 \log \left(\frac{p'_{\text{rms}}}{p_{\text{ref}}} \right). \tag{6}$$

We can notice (Fig. 4) that the Root Means Square (RMS) sound pressure level decreases from 100 dB near the speaker to about 86 dB at a distance of 1.2 m, what corresponds to the acoustic pressure changes from 2 Pa to about 0.4 Pa. Two vortices are formed in the center of the cavity where SPL reaches the lowest value of 72 dB. The trailing edge and the left bottom corner of the cavity are the places of the highest sound pressure level.
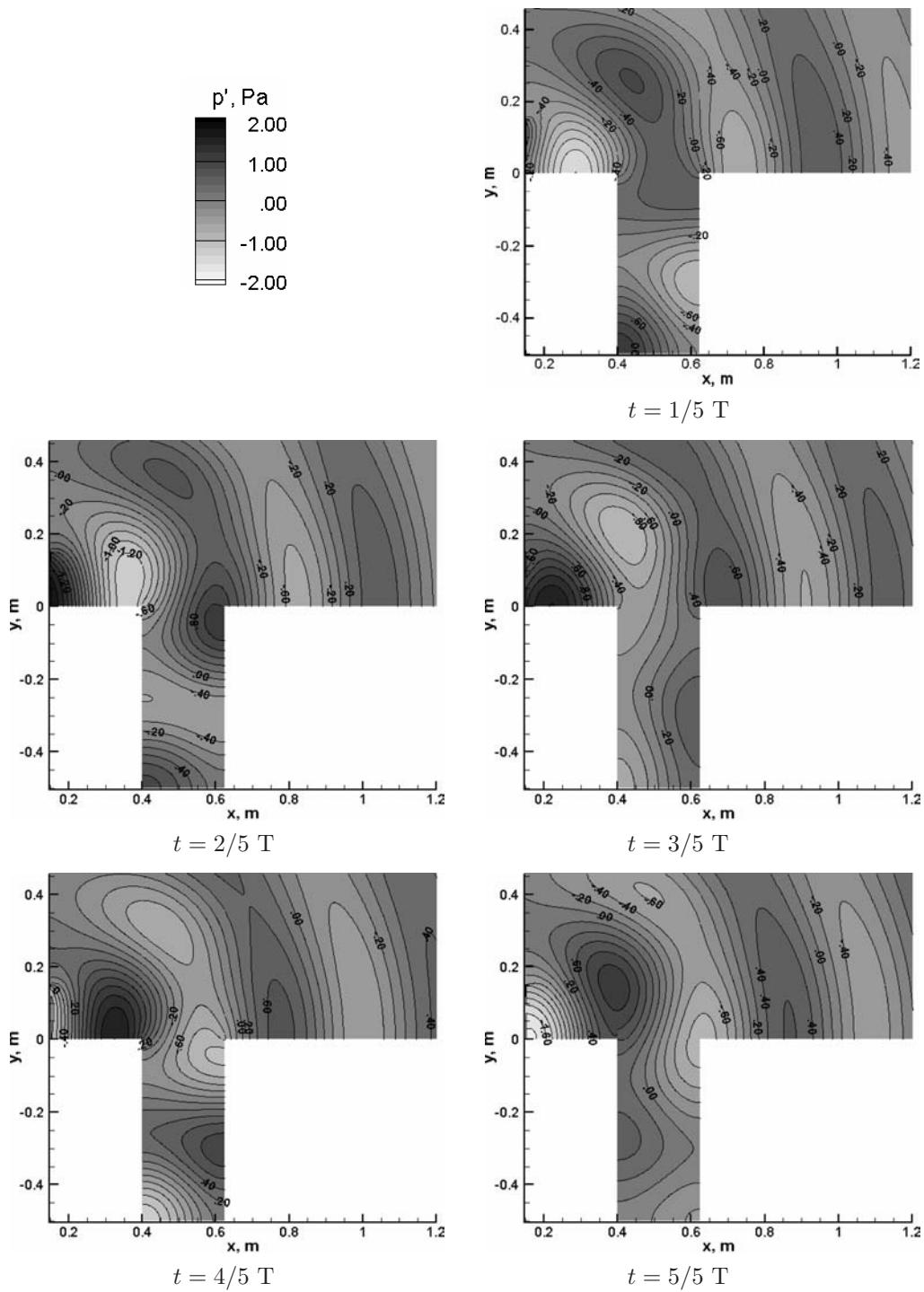
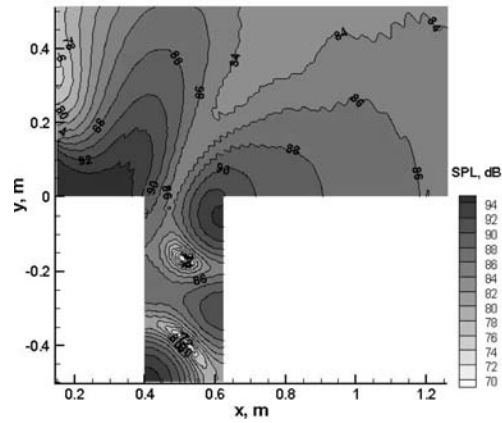Fig. 3. Five instantaneous states of acoustic wave emitted by a speaker and cavity.

Fig. 4. Sound pressure level distribution.

Figure 5 shows the acoustic pressure distribution in function of the distance for one instantaneous state $t = 5/5$ T. We can observe that the amplitude of the acoustic wave in this case extinguishes gradually and reaches a value of about 20% of the initial amplitude at a distance of 2 m.
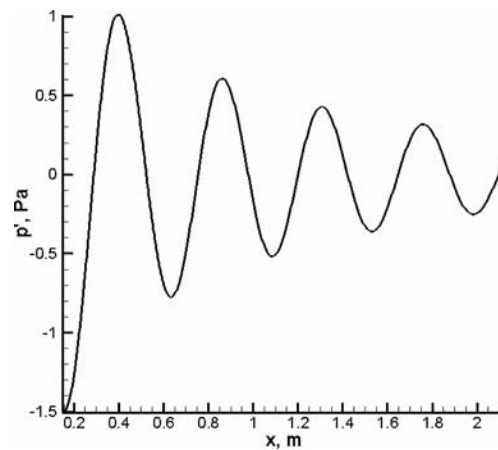

Fig. 5. Instantaneous acoustic pressure fluctuations in function of distance close to the bottom of the wall.

This phenomenon was experimentally investigated by WEYNA (2005), and the results presented in this paper are qualitatively consistent with experiments. In the work of WEYNA (2005) many experiments have been presented, which are very suitable for a thorough analysis of the acoustic waves numerical modeling, and can be used for further validation of the applied method.

Another problem in the aero-acoustic calculations is an identification of the aerodynamic noise on the basis of unsteady flow field data. This unsteadiness can be caused by a high level of turbulence in the flow or unsteady boundary

conditions, what can be solved similarly to the previous cases. The idea of the numerical method, which is based on the CAA model (2) and arbitrary CFD solution, consists in determination of the noise level in the internal as well as external flow structures independently of the CFD method.

During the iteration process (integration in time of Eqs. (2)) with global time step Δt, adequate states of the unsteady mean flow (vector $\mathbf{Q}_0$) are assumed. It means that the values of the $\mathbf{Q}_0$ are changing in time when the mean flow is unsteady. The accuracy of the acoustic field solution depends on the number of instantaneous states and the accuracy of the mean flow field computations (turbulence model, grid resolutions, etc.).

Among the hybrid LES/uRANS CFD methods, the calculations with a SAS turbulence model are the most promising with respect to the computational time and stability. However, using it for prediction of the acoustic parameters for a complicated 3D geometry, still requires a very fine mesh and a lot of computational time. Therefore, it seems advisable to use the simplest method, that would allow to obtain the acoustic data both in the near and far field by means of relatively simple and fast method. For this reason, one can use e.g. the Euler acoustic postprocessor (EAP).

For the domain presented in Fig. 6, the CFD calculations by means of SAS and uRANS model were performed. The test case is based on the experiment done by JACOB et al. (2002). The flow with Ma$\sim$0.2 around the cylinder and aerofoil was used for aerodynamic noise assessment.
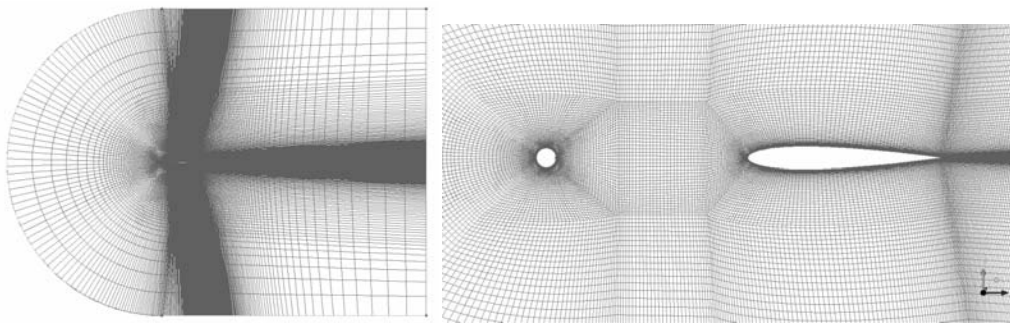

Fig. 6. Numerical grid near the cylinder and airfoil.

The time-dependent pressure distribution on the solid bodies, on the cylinder and profile in the selected case, can be used as the boundary condition in the method. The numerical mesh was created to preserve at least 10 mesh points per acoustic wavelength, that is satisfactory for the used method and has been proved in our former works.

Figure 7 shows the acoustic pressure distributions for SAS calculations and for the calculations made by means of EAP for the pressure distributions on the solid bodies taken from SAS results. It can be observed that for the SAS results, the

ANSYS CFX results with SAS turbulence model   Euler acoustic postprocessor results
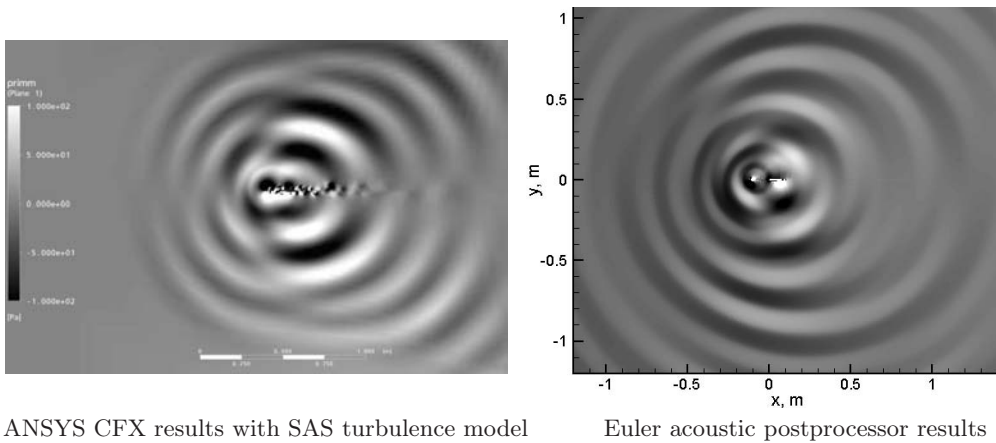
Fig. 7. Snapshot of the acoustic pressure distributions.

acoustic waves vanish due to the coarse grid in the far field region. The shape of the acoustic waves, that is similar to the shape of the outer boundary, shows that ANSYS CFX suffer from the accuracy in modelling of the non-reflective boundary conditions. The relatively coarse grid for EAP allows modelling of acoustic waves propagation in both near and far field, in reasonable time period.

Figure 8 presents the whole calculation domain for EAP simulations with marked points for near and far field analysis. The size of the used uniform numerical mesh is about 100.000 nodes. One can observe in this figure the satisfactory accuracy of the modelled acoustic waves and proper behaviour of the used non-reflective boundary conditions. In the description of the experiment it has been mentioned that far field SPL at 90 degrees was about 110.7 dB ($\pm$ 0.5 dB) (Jacob *et al.*, 2002).

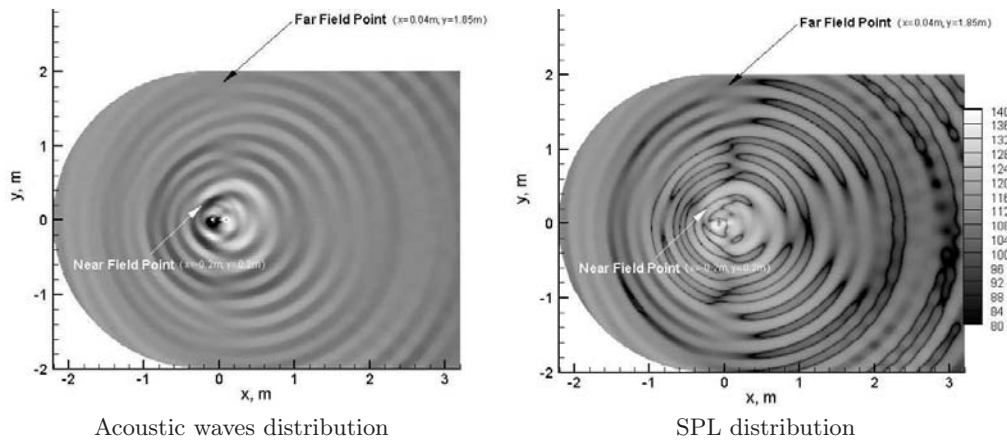Acoustic waves distribution   SPL distribution

Fig. 8. Snapshot of the acoustic pressure distribution and SPL for EAP calculations.

The near field point has been used to compare the EAP calculations with the prediction of the flow field carried out by CFD simulation with the SAS turbulence model. However, in the far field point, the numerical results of the EAP calculations have been compared with the experimental data of SPL spectrum (JACOB *et al.*, 2002). The far field point position corresponds to the coordinates $x = 0.04$ m and $y = 1.85$ m in the calculation domain and is located very closely to the outer boundary. At all the outer boundaries, the non-reflective boundary conditions have been applied.

The comparison of the SPL spectrum in the near field point (monitor point 1) between CFD calculations with the SAS turbulence model and EAP calculations has been presented in Fig. 9. The calculated SPL spectrum by means of EAP method is very close to the results obtained from the SAS calculations. It shows that EAP can be used for modelling of the aerodynamic noise in near field only, on the basis of pressure data on the cylinder and profile. It is important, because the time-consuming CFD modelling can be limited to the calculation domain as small as possible. The further CAA modelling could be performed for larger domain on a relatively coarse grid.
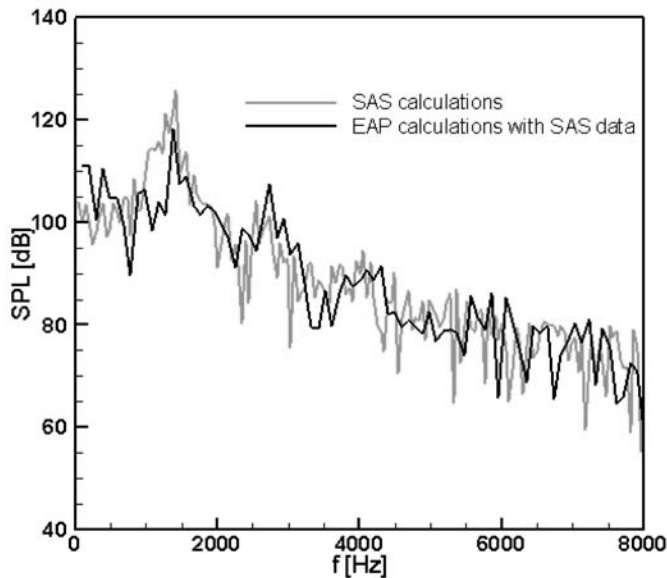

Fig. 9. SPL spectrum comparison in the near field in the monitor point 1.

Figure 10 shows the comparison of the SPL spectrum for the far field point. The EAP calculations with the pressure data on the solid bodies obtained from SAS and uRANS simulations have been compared with experimental data. The EAP with SAS data determine the main frequency and the SPL correctly, but the agreement with experiment is not satisfactory. It can be caused by the closeness
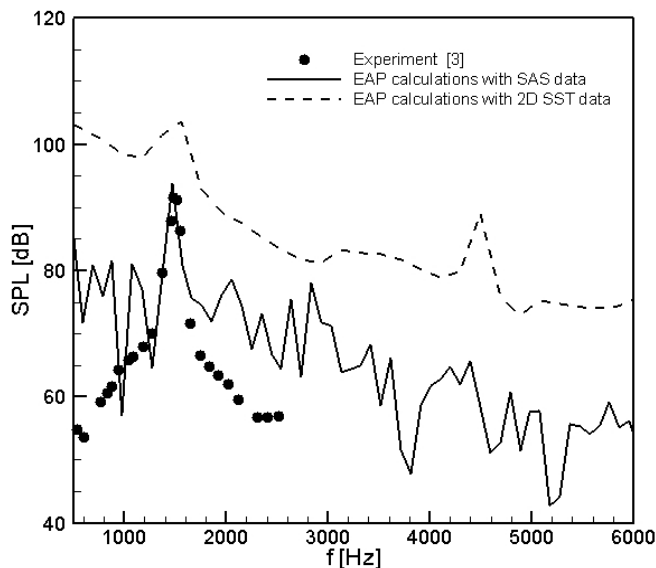
Fig. 10. SPL spectrum for the point in the far field.

of the far field point with the outer boundary. The EAP with uRANS data overestimates the SPL values and captures only the main frequencies.

4. Conclusions and future works

The paper presents a step towards the development of the CFD/CAA methods for modeling of the acoustic waves propagation and their generation. The full non-linear Euler equations for acoustic fluctuations are solved in order to predict the near field noise level and noise propagation in the mean flow. The presented Euler acoustic postprocessor (EAP) may be coupled with external, arbitrary CFD solver.

In the paper, the validation tests of the applied CAA method for an acoustic waves propagation were presented. The comparison with analytical solution for the Gaussian distribution pulse has been done. It has been proved that for the presented CAA method, the numerical mesh has to include at least 5 points per wave length.

Moreover, the influence of the solid boundary conditions for the acoustic waves propagation has been investigated. To this end, the interaction of the acoustic waves with the cavity has been tested.

Finally, the calculations of the aerodynamic noise in the flow around cylinder and aerofoil were performed. For unsteady pressure distributions on the solid bodies (cylinder and profile) the EAP was successfully used to assess the aerodynamic noise.

The elaborated method is an efficient tool for noise propagation modeling, including predictions of a pure acoustic waves distribution or modeling of the noise generated by unsteady flow field.

Further research will be concentrated on investigations of sensitivity of the elaborated method and validation of the presented hybrid CFD/CAA method against the experimental data. An application of this method for identification of the acoustic sources, places and intensity will be also a subject of our intensive research.

Acknowledgments

References

1. Dykas S., Wróblewski W., Chmielniak T. (2006a), *Numerical modeling of noise with the use of URANS and Euler methods*, Chemical and Process Engineering J., **27**, 626–694.

2. Dykas S., Wróblewski W. (2006b), *A method for aerodynamic noise modeling in the transonic flows* [in Polish: *Metoda modelowania hałasu aerodynamicznego w przepływach okołodzwiekowych*], Wyd. Politechniki Śląskiej, Gliwice.

3. Dykas S., Wróblewski W., Chmielniak T. (2008), *Aerodynamic noise assessment using a CFD/CAA technique*, Proc. of ASME, Berlin 2008, GT2008-50140.

4. Jacob M.C., Boudet J., Casalino D., Michard M. (2002), *A rod-airfoil experiment as benchmark for broadband noise modeling*, 3rd SWING Aeroacoustic Workshop, Stuttgart.

5. Prantle I. (2002), *The aeroacoustics on the basis of acoustic analogies with LES and URANS* [in German: *Strömungsakustik auf der Basis akustischer Analogie mit LES und URANS*], PhD Thesis, Universität Karlsruhe, 2002.

6. Sorgüven E. (2004), *A Computational Aeroacoustic Method Using Large Eddy Simulation and Acoustic Analogy*, PhD Thesis, Universität Karslruhe.

7. Tam C.K.W. (1995), *Computational Aeroacoustics: Issues and Methods*, AIAA Journal, **33**, 10, 1788–1796.

8. Weyna S. (2005), *An acoustic energy dissipation of the real sources* [in Polish: *Rozpływ energii akustycznych źródeł rzeczywistych*], Wydawnictwa Naukowo-Techniczne.